Mineral coatings for temporally controlled delivery of multiple proteins

Jae Sung Lee,
Department of Biomedical Engineering, University of Wisconsin, 1550 Engineering Drive, Madison, WI 53706 (USA)

Darilis Suarez-Gonzalez, and
Materials Science Program, University of Wisconsin, 1509 University Avenue, Madison, WI 53706 (USA)

William L. Murphy
Department of Biomedical Engineering, University of Wisconsin, 1550 Engineering Drive, Madison, WI 53706 (USA)

Department of Orthopedics and Rehabilitation, University of Wisconsin, 600 Highland Avenue, Madison, WI 53792 (USA)

Department of Pharmacology, University of Wisconsin, 1300 University Avenue, Madison, WI 53706 (USA)

Collaborative Research Center, AO Foundation

William L. Murphy: wlmurphy@wisc.edu

Keywords

biomimetics; drug delivery; functional coatings; medical applications; tissue engineering

Calcium phosphate (CaP) materials have been widely used as bone substitutes in dentistry and orthopedics, since they bear compositional and functional similarity to human teeth and bones.[1] Clinically relevant examples of CaP materials include hydroxyapatite (HAP, $Ca_{10}(PO_4)_6(OH)_2$), β-tricalcium phosphate (β-TCP, β-$Ca_3(PO_4)_2$) and biphasic calcium phosphate (BCP) composed of HAP and β-TCP. These materials have been a subject of considerable academic and industrial interest owing to their "osteoconductive" properties.[2] Specifically, CaP materials improve integration of biomaterials with surrounding bone tissue, and further serve as a template for proper function of bone-forming cells. The favorable aspects of CaP materials have led to their extensive clinical use as bone void fillers,[3] and as coating materials on various implants to promote bone-implant bonding.[4] However, the pro-osteogenic ability of CaP is often insufficient for the structural and functional restoration of bone tissue, particularly in large bone defects. Therefore, there has been a growing demand to deliver biologically active proteins, such as growth factors,

cytokines, and antibodies, which can actively guide cellular response toward new bone formation.[5]

Natural bone development and healing are orchestrated by a cascade of numerous biologically active proteins.[6] However, current clinical strategies for delivery rely on bolus delivery of a single protein, most notably the growth factor bone morphogenetic protein-2 (BMP-2), via collagen sponges, where the rapid release of high dose protein has led to safety concerns related to edema and heterotopic bone formation.[7] Poorly controlled delivery kinetics may also diminish the therapeutic efficacy of bone growth factors like BMP-2, since they may be more effective when delivered in a temporally regulated manner that mimics natural bone healing. Controlled release kinetics have in fact been demonstrated in particulate delivery carriers and scaffold constructs by modulating their molecular architecture and structural characteristics.[8] However, their clinical application to functional musculoskeletal healing may be practically limited, since they do not represent a stand-alone device for tissue ingrowth or their fabrication conditions are not appropriate to include biologically active proteins. Furthermore, there is an increasing need for sophisticated delivery systems capable of delivering multiple growth factors to induce cooperative, synergistic healing processes that mimic natural wound healing (e.g., angiogenesis and neurogenesis).[9] In view of this opportunity, recent studies have focused on protein encapsulation in multi-component polymer scaffolds as a mechanism for sustained release of multiple proteins.[10] These studies have demonstrated that it is possible to deliver multiple therapeutic proteins with distinct release kinetics, with clear consequences for new tissue formation. Multiple protein release could be particularly advantageous if it could be achieved from the surface of common medical devices without negatively influencing bulk device properties.

In light of the need for timed delivery of multiple proteins from standard orthopedic and dental devices, here we use thin, resorbable CaP coatings to achieve temporally controllable delivery of multiple proteins. Our general approach involves growing a carbonate-substituted hydroxyapatite (cHAP, $Ca_{10-x}(PO_4)_{6-x}(CO_3)_x(OH)_{2-x}$[11]) coating on a base material via a biomimetic process,[12] followed by binding a protein of interest to the cHAP coating via a process that mimics hydroxyapatite chromatography (Figure 1).[13] We hypothesized that the physicochemical properties of cHAP coating (i.e., morphology and dissolution rate) could be changed by varying the cHAP coating conditions, and that the coating could continue to grow after initial protein binding to the coating. Specifically we hypothesized that; (i) the dissolution rate of the cHAP coating would influence the protein release rate, leading to controllable release rates; and (ii) the insertion of multiple proteins into the cHAP layer at varying stages of its growth would lead to temporally controlled release of multiple proteins. In this initial study, we demonstrated this concept using β-TCP as a base material, as it is currently used as a bone void filling material in widespread orthopedic and dental applications, in which controlled protein release could be particularly important.[14]

First, we incubated porous β-TCP granules in modified simulated body fluid (mSBF; 141 mM NaCl, 4 mM KCl, 0.5 mM $MgSO_4$, 1.0 mM $MgCl_2$, 4.2 mM $NaHCO_3$, 5.0 mM $CaCl_2$, 2.0 mM KH_2PO_4, 20 mM Tris base) for 7 days to create a continuous cHAP coating on a β-

TCP substrate. The mSBF has ionic composition similar to that of human blood plasma except doubled calcium and phosphate ions, and has been used to create biomimetic cHAP coatings in several previous studies from us and others.[15, 16, 17, 18] Supersaturated calcium and phosphate ions in mSBF can induce mineral nucleation on negatively charged phosphate sites on the β-TCP surface, and subsequent growth of CaP mineral crystals (Figure S1 in supporting information). Carbonate ions in mSBF can, in general, substitute the phosphate ions, hydroxyl ions or both in the CaP crystal lattice, although carbonate substitution is known to occur in various modes via anionic and cationic substitutions. The mSBF incubation of β-TCP materials produced a nanoporous, plate-like cHAP coating (pore size: 168 ± 14 nm) on the entire surface (Figure 2a). Energy dispersive X-ray spectroscopy (EDS) showed that the calcium/phosphorus ratio of the surface was changed from 1.56 in the uncoated β-TCP (Figure S2) to 1.66 (inset of Figure 2a) due to the presence of the cHAP coating layer. Fourier transform infrared spectroscopy (FT-IR) displayed sharpened characteristic peaks associated with phosphate and carbonate after cHAP coating (Figure S3). Importantly, the presence of the cHAP coating stabilized the β-TCP substrate in aqueous conditions, and significantly slowed the dissolution rate of the β-TCP material (Figure 2b). The cHAP is less soluble in aqueous solution than β-TCP, as the solubility product (K_{sp}) of cHAP and β-TCP are 2.88×10^{-112} M$^{18[19]}$ and 1.26×10^{-29} M$^{5[20]}$, respectively, which were experimentally determined by measuring the dissolved ion concentrations in aqueous solution at 37 °C. Therefore, we hypothesize that cHAP coatings serve as a protective layer by shielding the β-TCP surface from the surrounding solution. In addition, nanoporous cHAP coating can locally generate high calcium and phosphate concentrations around β-TCP, resulting in retarded dissolution of β-TCP. These factors each likely contributed to the improved stability of β-TCP after cHAP coating. Although it was not the specific goal of this study, this stabilization effect may be important, as the relatively fast resorption rate of β-TCP relative to other calcium phosphate minerals is a drawback in some clinical applications. The cHAP coatings provide a mechanism to controllably slow the dissolution rate of β-TCP devices.

We examined protein binding to cHAP coatings by incubating cHAP-coated β-TCP granules in phosphate-buffered saline (PBS) solutions of various BSA concentrations. The amount of BSA binding was proportional to BSA concentration up to 1000 μg mL^{-1}, with the highest binding capacity of 0.52 ± 0.04 μg mg^{-1} β-TCP (Figure 2c). When compared to the initially added BSA in the solution, 16.0 ± 2.1 % of proteins were bound to the cHAP-coated β-TCP granules. The protein binding capacity on coated β-TCP was enhanced by over 3-fold when compared to that of the uncoated β-TCP (0.16 ± 0.01 μg mg^{-1} β-TCP) when incubated in the highest BSA concentration (1000 μg mL^{-1}) (Figure 2c). The increased binding may be due to the expanded surface area as a result of the nanoporous cHAP coating. The BSA release in PBS was rapid, with 82.7 ± 4.2 % of the initially bound BSA released within 10 days (Figure 2d). In addition, we performed another experiment releasing vascular endothelial growth factor (VEGF) in cell culture Dulbecco's modified Eagle medium (DMEM), which represents a more clinically pertinent condition. VEGF is a pro-angiogenic growth factor capable to induce the new vessel formation, a critical process in bone tissue repair. VEGF was incorporated on cHAP-coated β-TCP granules by incubating in a 1 μg mL^{-1} VEGF solution, and VEGF showed similar release behavior in DMEM to that of BSA in PBS.

Specifically, 80.8 ± 14.4 % of the initially bound VEGF was released within 13 days, with 33.0 ± 11.2 % released during the first day of release.

We next investigated the influence of additional mineral coating on the release rate of BSA. Here we bound BSA to an initial cHAP coating grown in mSBF with 4.2 mM carbonate, and then created an additional cHAP coating upon the initial BSA-bound coating. Specifically, cHAP-coated β-TCP granules were incubated in 1000 μg mL^{-1} BSA solution, and then subsequently incubated in mSBF solutions with different carbonate concentrations (4.2 and 100 mM) for different periods (0.5 and 5 day) to obtain additional cHAP coatings with varying degrees of carbonate substitution and microstructure. This additional mSBF incubation led to the formation of an additional cHAP layer, the structure of which became denser with a smaller pore size when it was created in mSBF with higher carbonate concentration for a longer time period (Figure 3a–d). Specifically, the average pore sizes were 146 ± 45 nm and 48 ± 16 nm when the additional coating was made for 0.5 day in mSBF with 4.2 and 100 mM carbonate, respectively. They were then decreased to 106 ± 34 and 38 ± 12 nm after 5-day incubation in mSBF solution with 4.2 and 100 mM carbonate, respectively. As expected, the ratio of calcium to phosphorus (Ca/P) was increased when cHAP coatings were grown in mSBF with higher carbonate concentration, consistent with carbonate substitution for phosphate ions. The Ca/P ratios were 1.64 ± 0.08 and 1.85 ± 0.03 for cHAP coatings formed in mSBF containing 4.2 mM carbonate for 0.5 and 5 days, whereas those of cHAP coatings in mSBF with 100 mM carbonate were 1.99 ± 0.18 and 2.00 ± 0.12. In order to validate the feasibility of this approach, it was important to confirm that the loss of protein during mineral coating process is insignificant. Thus, we quantified protein release during the additional mineral coating process and found that less than 2 % of the initially bound BSA was lost into the solution during the 5-day mSBF incubation (Figure 3e). It indicates that the BSA remained bound to the initial coating during subsequent, additional growth of the coating.

It is instructive to compare this result (i.e., release of less than 2 % of BSA in mSBF) to BSA release shown in Figure 2d, in which over 60 % of BSA was released in PBS from initial coatings. In the biomimetic mineralization process, mineral coating formation and dissolution are reversible, and their equilibrium is detennined by the degree of saturation of the surrounding solution. In general, mineral coatings can be formed when the surrounding environment is supersaturated with calcium and phosphate ions, whereas mineral coatings are dissolved in undersaturated conditions (i.e., lower [calcium] and [phosphate] in the solution). Therefore, a small amount of initially bound BSA was released in mSBF, in which mineral formation is favorable due to the supersaturated [calcium] and [phosphate]. In contrast, a larger quantity of initially bound BSA was released in PBS, where mineral dissolution is dominant due to the undersaturated [calcium] amd [phosphate]. Thus, protein release from cHAP mineral coatings is clearly influenced by the surrounding solution characteristics, and this has relevance to *in vivo* applications. An additional mechanism that may limit BSA release during the additional coating process could involve protein re-adsorption to cHAP that is continuously forming in the mSBF solution. However, this study demonstrates that it is possible to tune the release rate of multiple proteins by varying the

intrinsic mineral properties and the timing of protein incorporation into a growing mineral coating.

Importantly, BSA release kinetics were significantly slower (over 20 days) in all conditions that included an additional cHAP coating layer (Figure 3f) when compared to the condition in which there was no additional cHAP coating (~10 days, Figure 2d). The change in release kinetics was dependent on the characteristics of the additional cHAP coating. Higher carbonate content during formation of the additional mineral layer resulted in a higher initial release in the first 48 hours, followed by slower sustained release kinetics over more than 25 days (Figure 3f, circles vs. triangles). This initially higher release of BSA from coatings formed with higher carbonate content can be explained by the observation that the additional mineral coating formed from mSBF with 100 mM carbonate was less stable and dissolved more quickly due to higher carbonate substitution, as the carbonate substitution results in the disruption of crystal lattice and thus increased solubility of coating (Figure S4 and S5 in supporting information and[19, 21]). This accelerated release from mineral coating formed from mSBF with higher carbonate was not observed at later time points. To explain this release behavior, two aspects should be taken into consideration. One is the stability of mineral coating and the other is the surface area of mineral coating. The former would influence how quickly proteins are desorbed from the mineral surface, and the latter would affect the time needed for protein molecules to escape from mineral coating. We surmise that cHAP coatings formed from mSBF with 100 mM carbonate would dissolve to a higher degree, and the accelerated protein release due to mineral dissolution would dominate the effect of increased surface area, which would tend to retard protein release. However, the mineral phase of the coating surface might be altered to a more stable phase during the course of incubation due to reprecipitation of released calcium and phosphate ions. The reprecipitated coating surface would have lower degree of carbonate substitution because the reprecipitation would proceed in the presence of significantly less carbonate ions compared to when the initial coating was created in mSBF with 100 mM carbonate. This lower carbonate substitution would be expected to result in lower solubility.[19, 21] This effect would slow down mineral dissolution and lead to suppressed protein release at later time points, particularly on coatings with higher surface area.

On the other hand, the more stable outer coating prepared in mSBF containing 4.2 mM carbonate eliminated the "burst" release over the initial 48 hours. This result indicates that it is possible to limit burst release of protein by incorporating the protein into a cHAP mineral coating. Longer time durations of additional cHAP coating also resulted in slower release kinetics, regardless of the amount of carbonate present during additional coating growth (Figure 3f, filled symbols vs. open symbols). When the additional cHAP layer was prepared in mSBF for 5 days, initial burst release was avoided and BSA release was significantly delayed. This is likely attributable to the combination of the pore structure of additional cHAP layer and repetitive protein adsorption/desorption cycles. Specifically, the cHAP coating is highly nanoporous, and protein molecules bound deep inside the coating layers with smaller pores should experience a longer pathway to diffuse out from the coating layer. During the diffusion, the proteins would continuously face the cHAP surface and experience adsorption/desorption process repeatedly until they ultimately escape the coating layer, which would lead to delayed BSA release, as observed in this and previous studies.[16, 17]

To assess the ability to deliver multiple proteins in a temporally controlled manner, we incorporated BSA on the initial cHAP mineral layer, formed an additional coating layer, then bound lysozyme on the additional cHAP coating (formed in mSBF containing 4.2 mM carbonate for 0.5 day) (Figure 4a). Consequently, BSA was encapsulated between the initial and additional cHAP coating, and lysozyme is bound on the additional cHAP coating. The release profiles for these two proteins were dramatically different. The majority of lysozyme (79.5 ± 8.7 %) was released within the first 5 days while 61.4 ± 8.0 % of BSA was released in a sustained manner over 27 days (Figure 4b). Interestingly, the release profiles of BSA and lysozyme from coatings during simultaneous release closely reflected the release of each protein incorporated alone at the identical stage of coating formation in the layered cHAP coatings. Thus, release behavior of each protein from cHAP coatings is not altered by the presence of another protein species, and presence and choice of cHAP coating may enable the release of multiple proteins with independent release profiles in a temporally predictable manner.

In summary, we developed a temporally controllable protein delivery system on a common orthopedic device material, β-TCP, using tunable cHAP coatings. Release of protein molecules was controlled by modulating the dissolution rate and nanostructure of an outer cHAP layer. Results indicated that exterior cHAP coating layers with slower dissolution rates and denser structures consisting of smaller pores resulted in sustained protein release with reduced initial burst release. Dual protein release with distinct and independently predictable release profiles was achieved by binding proteins at the different stages of cHAP coating formation. It should be noted that, although here we mainly focus on binding and release of model proteins, our previous studies have demonstrated that similar cHAP coatings can deliver various biologically active growth factors such as fibroblast growth factor-2 and BMP-2, and promote orthopedic tissue repair *in vivo* animal models.[17, 22] This approach may be attractive in medical device design, as the thin cHAP coatings provide controllable delivery of one or more therapeutic proteins while maintaining key bulk device properties. It is noteworthy that extension of this approach to sequential multi-protein delivery may provide a further mechanism for independent regulation of early-stage and late stage processes during tissue formation. In particular, this approach may be relevant in bone tissue engineering approaches, in which short-term release of pro-angiogenic factors and long-term release of pro-osteogenic factors is desirable. In addition, in view of previous studies in which similar cHAP coatings have been created on various medical device platforms (e.g. surgical sutures,[17] bone screws,[18] microspheres,[23] polymer scaffolds,[24] hydrogels[25]), the approach described here may provide a generally applicable method to deliver multiple proteins in a temporally controlled manner in clinical applications.

Experimental

Formation of cHAP coating

β-TCP granules (particle size: 3–6 mm, average pore size: 250 μm; Berkeley Advanced Biomaterials, Berkeley, CA) were incubated in mSBF with 4.2 or 100 mM NaHCO$_3$ to create cHAP coatings. Each granule was incubated in at least 10 mL of mSBF to ensure the constant ionic concentration during coating formation. All initial cHAP coatings were grown

in mSBF containing 4.2 mM $NaHCO_3$ for 7 days at pH 6.8 and 37 °C. In another set of experiments, additional coatings were created on the initial cHAP coating by incubating in mSBF with different carbonate concentrations, 4.2 or 100 mM $NaHCO_3$, for different times 0.5 and 5 days. The incubations were performed at pH 6.8 and 37 °C with gentle rotation with mSBF being refreshed daily. Proteins were bound after initial coatings were produced, after additional coatings were formed, or both.

Characterization of cHAP coating

Morphological and elemental analysis of cHAP coating was carried out using LEO 1530 field emission scanning microscopy (FE-SEM; Zeiss, Germany) and EDS equipped on FE-SEM, respectively. FT-IR was performed by Equinox 55 spectrometer (Bruker AXS, Germany) using palletized samples with potassium bromide. ImageJ software (National Institutes of Health, Bethesda, MD) was used to estimate the pore size of cHAP coatings from SEM images.

Protein incorporation to cHAP coating

Each of cHAP-coated β-TCP granules (30–70 mg) was incubated in 200 μL protein solution in PBS at 37 °C for 4 hours to allow for protein incorporation. After binding, the protein concentration in the remaining solution using microBCA protein assay (Pierce, Rockford, IL), and the amount of bound protein was calculated from the protein concentration change before and after binding. The data shown were normalized to the mass of sample.

Dissolution of cHAP-coated or uncoated β-TCP granule

We assessed the calcium release as a measure of dissolution of cHAP coating or β-TCP granule. Each of the samples was incubated in 200 μL of PBS (pH 7.4) at 37 °C in a static condition without agitation, and at each time point the amount of calcium in the incubating media was measured using colorimetric assay using arsenazo III (MP Biochemicals, Solon, OH). All data were normalized to the mass of the sample.

Protein release from cHAP-coated β-TCP granule

After rinsing, each of protein-incorporated, cHAP-coated β-TCP granules was incubated in 200 μL of PBS (pH 7.4) at 37 °C and at indicated time points, the amount of protein released in the release media was measured using colorimetric microBCA assay or fluorescence assay. At each time point, release medium was collected and replaced with fresh PBS to ensure sink conditions during release of protein molecules. In another experiment, we incorporated carboxyfluorescein-labeled BSA to cHAP-coated β-TCP granules and determined the protein release in mSBF during additional mineral coating. All protein release experiments were performed in a static condition. The data are shown as the amount of protein normalized to the mass of the sample, or as the percentage of the protein amount initially incorporated within cHAP-coated β-TCP granules.

Supplementary Material

Refer to Web version on PubMed Central for supplementary material.

Acknowledgements

References

1. a) Hak DJ. J. Am. Acad. Orthop. Surg. 2007; 15:525. [PubMed: 17761609] b) Jarcho M. Dent. Clin. North Am. 1986; 30:25. [PubMed: 3514291] c) Tay BKB, Patel VV, Bradford DS. Orthop. Clin. North Am. 1999; 30:615. [PubMed: 10471766]

2. a) Dorozhkin SV. J. Mater. Sci. 2008; 43:3028.b) Dorozhkin SV, Epple M. Angew. Chem. Int. Edit. 2002; 41:3130.c) LeGeros RZ. Clin. Orthop. Relat. Res. 2002; 395:81. [PubMed: 11937868]

3. Hing KA, Wilson LE, Buckland T. Spine J. 2007; 7:475. [PubMed: 17630146]

4. a) Cook SD, Thomas KA, Kay JF, Jarcho M. Clin. Orthop. Relat. Res. 1988; 232:225. [PubMed: 2838208] b) Le Guehennec L, Soueidan A, Layrolle P, Amouriq Y. Dent. Mater. 2007; 23:844. [PubMed: 16904738]

5. Kanczler JM, Oreffo ROC. Eur. Cells Mater. 2008; 15:100.

6. a) Braddock M, Houston P, Campbell C, Ashcroft P. News Physiol. Sci. 2001; 16:208. [PubMed: 11572922] b) Tsiridis E, Upadhyay N, Giannoudis P. Injury. 2007; 38:S11. [PubMed: 17383481]

7. a) Shields LBE, Raque GH, Glassman SD, Campbell M, Vitaz T, Harpring J, Shields CB. Spine. 2006; 31:542. [PubMed: 16508549] b) Wong DA, Kumar A, Jatana S, Ghiselli G, Wong K. Spine J. 2008; 8:1011. [PubMed: 18037352]

8. a) Cohen S, Yoshioka T, Lucarelli M, Hwang LH, Langer R. Pharm. Res. 1991; 8:713. [PubMed: 2062800] b) Kim HW, Knowles JC, Kim HE. J. Biomed. Mater. Res. Part B. 2004; 70B:240.c) Leong KW, Kost J, Mathiowitz E, Langer R. Biomaterials. 1986; 7:364. [PubMed: 3778996] d) Pekarek KJ, Jacob JS, Mathiowitz E. Nature. 1994; 367:258. [PubMed: 8121490]

9. Chen FM, Zhang M, Wu ZF. Biomaterials. 2010; 31:6279. [PubMed: 20493521]

10. a) Kempen DHR, Lu LC, Heijink A, Hefferan TE, Creemers LB, Maran A, Yaszemski MJ, Dhert WJA. Biomaterials. 2009; 30:2816. [PubMed: 19232714] b) Wang XQ, Wenk E, Zhang XH, Meinel L, Vunjak-Novakovic G, Kaplan DL. J. Control. Release. 2009; 134:81. [PubMed: 19071168]

11. Montel G, Bonel G, Heughebaert JC, Trombe JC, Rey C. J. Cryst. Growth. 1981; 53:74.

12. Liu YL, Wu G, de Groot K. J. R. Soc. Interface. 2010; 7:S631. [PubMed: 20484228]

13. Bernardi G, Kawasaki T. Biochim. Biophys. Acta. 1968; 160:301. [PubMed: 5680264]

14. a) Laffargue P, Fialdes P, Frayssinet P, Rtaimate M, Hildebrand HF, Marchandise X. J. Biomed. Mater. Res. 2000; 49:415. [PubMed: 10602075] b) Lind M, Overgaard S, Soballe K, Nguyen T, Ongpipattanakul B, Bunger C. J. Orthop. Res. 1996; 14:343. [PubMed: 8676246]

15. a) Choi S, Murphy WL. Acta Biomater. 2010; 6:3426. [PubMed: 20304109] b) Kokubo T, Kim HM, Kawashita M. Biomaterials. 2003; 24:2161. [PubMed: 12699652]

16. Jongpoiboonkit L, Franklin-Ford T, Murphy WL. Adv. Mater. 2009; 21:1960.

17. Lee JS, Lu Y, Baer GS, Markel MD, Murphy WL. J. Mater. Chem. 2010; 20:8894.

18. Lu Y, Markel MD, Nemke B, Lee JS, Graf BK, Murphy WL. Arthroscopy. 2009; 25:1427. [PubMed: 19962070]

19. Tang RK, Henneman ZJ, Nancollas GH. J. Cryst. Growth. 2003; 249:614.

20. Gregory TM, Moreno EC, Patel JM, Brown WE. J. Res. Nat. Bur. Stand. Sect. A. 1974; 78A:667.

21. Barralet J, Akao M, Aoki H, Aoki H. J. Biomed. Mater. Res. 2000; 49:176. [PubMed: 10571903]

22. Lee JS, Lee JS, Murphy WL. Acta Biomater. 2010; 6:21. [PubMed: 19665062]

23. Jongpaiboonkit L, Franklin-Ford T, Murphy WL. ACS Appl. Mater. Interfaces. 2009; 1:1504. [PubMed: 20161578]

24. Murphy WL, Kohn DH, Mooney DJ. J. Biomed. Mater. Res. 2000; 50:50. [PubMed: 10644963]

25. Suarez-Gonzalez D, Barnhart K, Saito E, Vanderby R, Hollister SJ, Murphy WL. J. Biomed. Mater. Res. Part A. 2010; 95A:222.
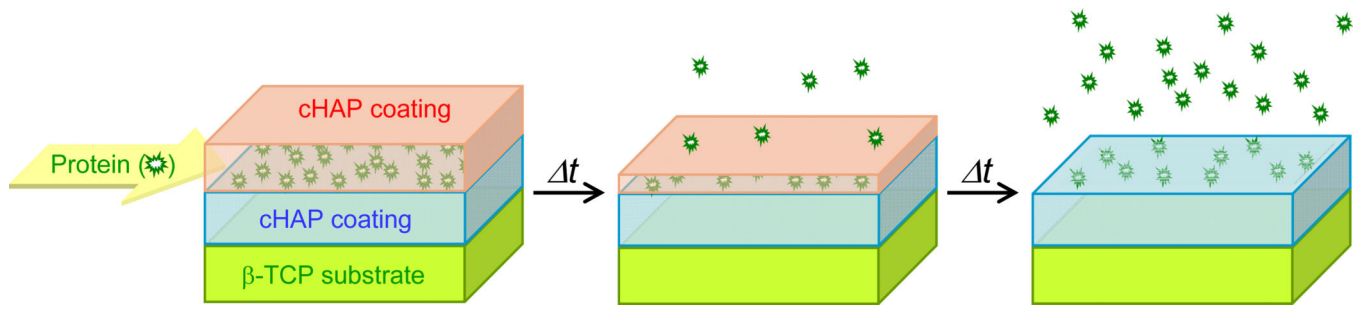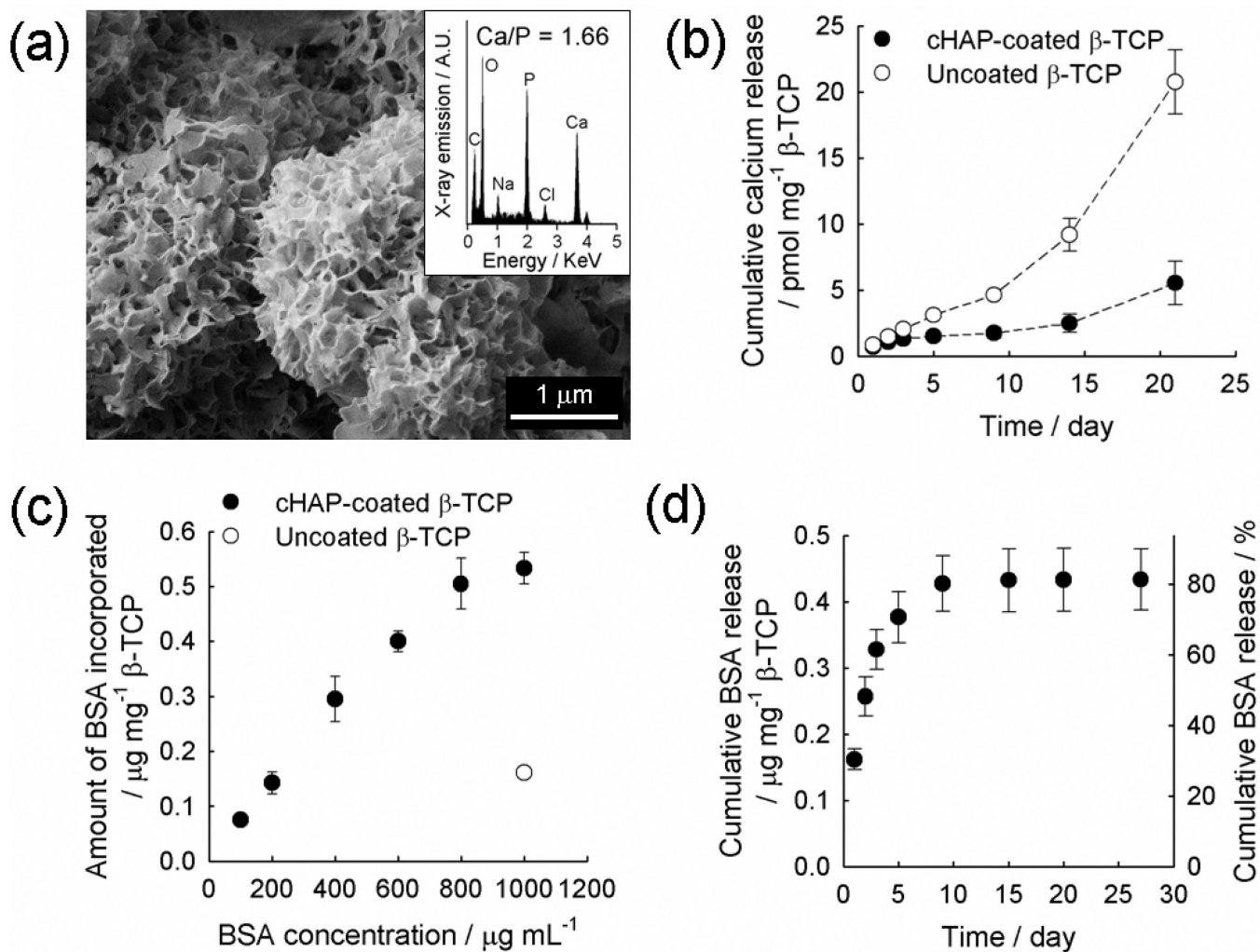
Figure 1.
Schematic illustration of temporally controllable protein delivery system created on a β-TCP material using layered cHAP coatings, and its evolution over the course of time.

Figure 2.
(a) SEM image and EDS spectrum (inset) of a cHAP-coated β-TCP granule, (b) cumulative calcium release from cHAP-coated and uncoated β-TCP granules, (c) binding profile of BSA on cHAP-coated and uncoated β-TCP granules, and (d) cumulative BSA release from cHAP-coated β-TCP granules in the absence of an additional coating.
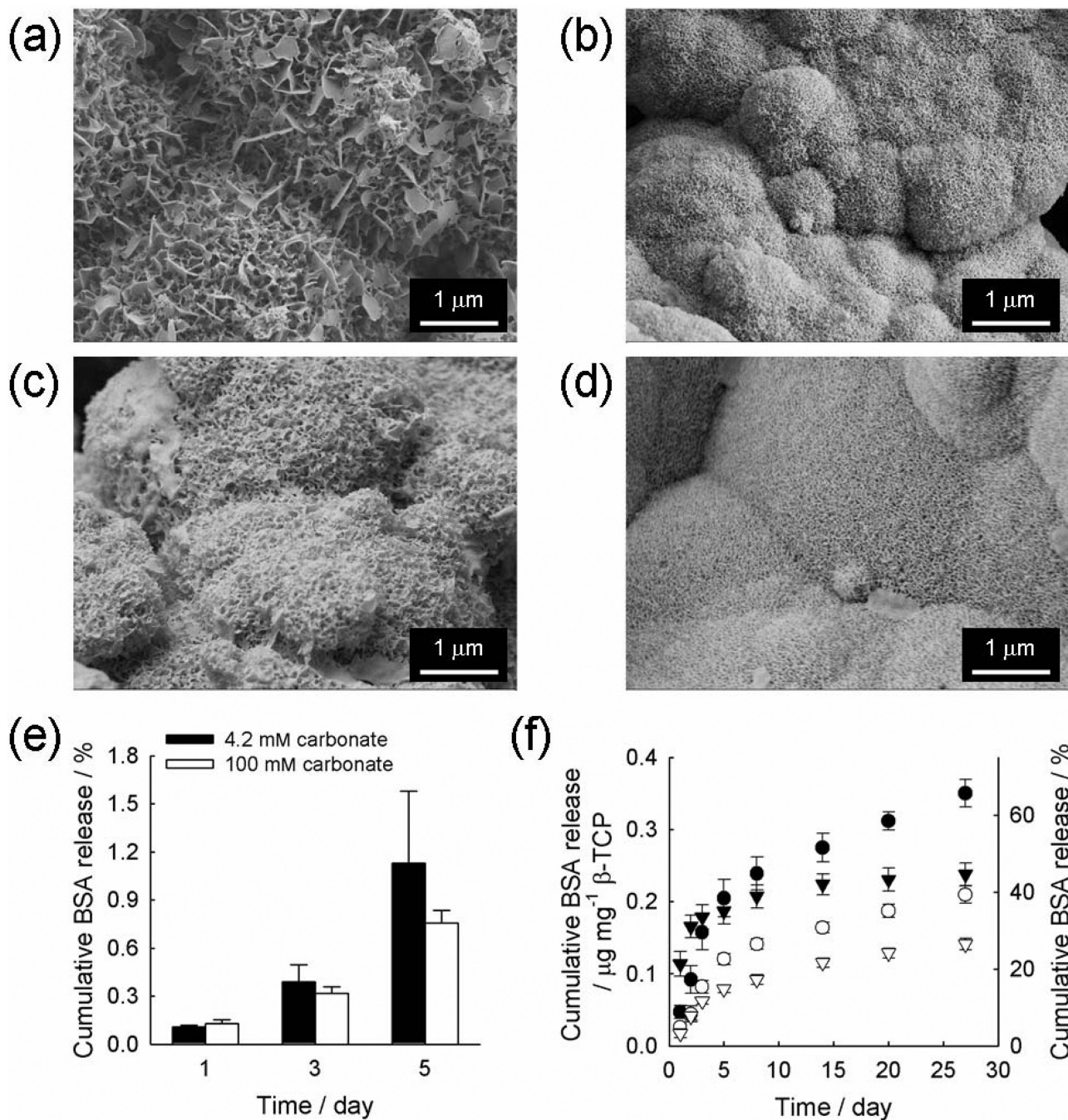
Figure 3.
SEM images of additional cHAP coatings created on BSA-bound, cHAP-coated β-TCP granules. Additional coatings were formed by incubating in mSBF with 4.2 (a, c) or 100 mM (b, d) carbonate for 0.5 (a, b) or 5 days (c, d). (e) Cumulative BSA release from BSA-bound cHAP coatings during additional cHAP coating formation in mSBF with different carbonate concentrations. (f) Cumulative BSA release from layered cHAP coatings formed on β-TCP granules, where an additional coating layer was created by incubating in mSBF

with different carbonate concentrations, 4.2 (circles) and 100 mM (triangles), for different time periods, 0.5 (filled symbols) and 5 day (open symbols).
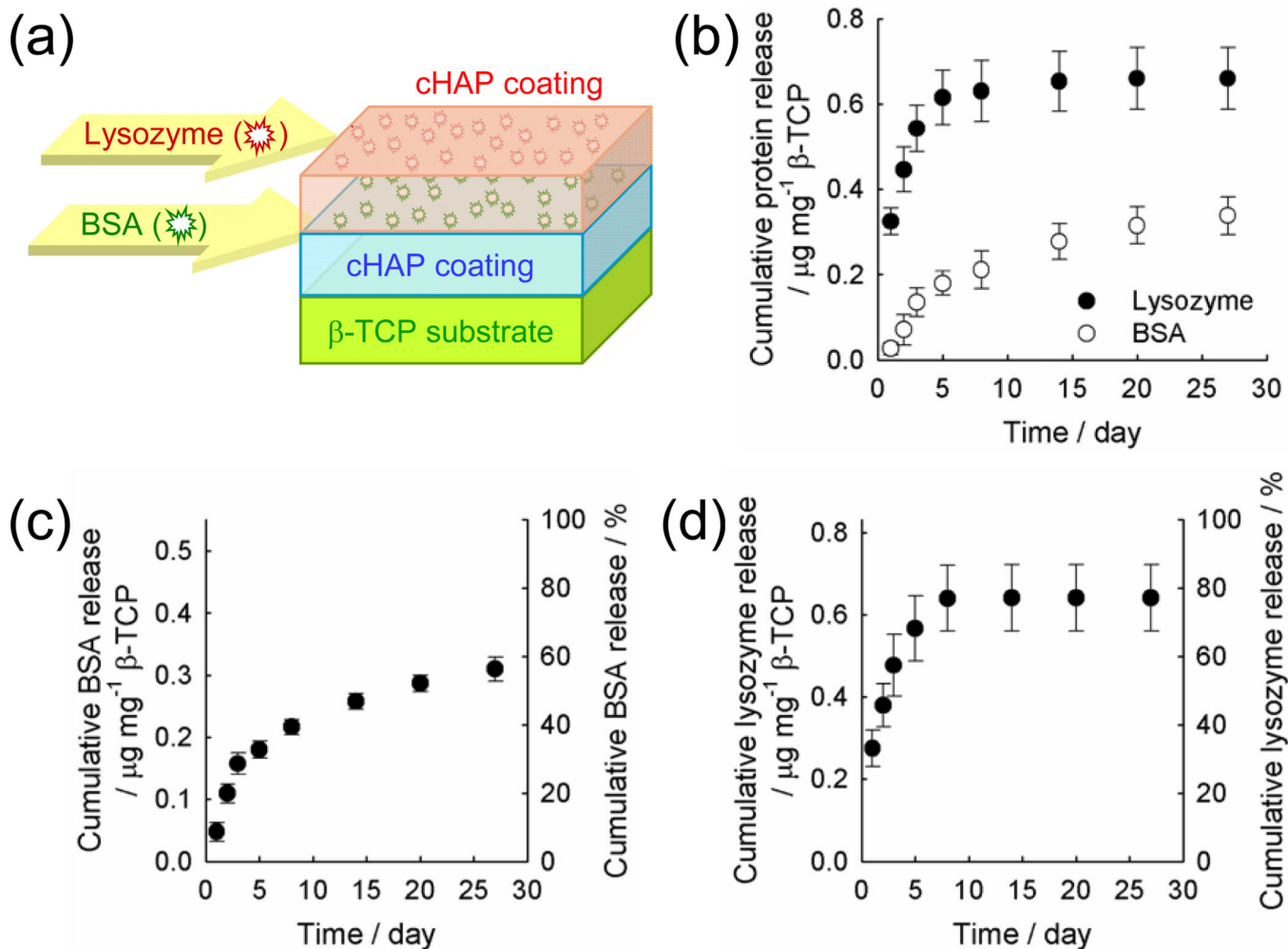
Figure 4.
(a) Schematic illustration of dual protein delivery system using layered cHAP coatings. BSA was encapsulated between cHAP coatings and lysozyme was bound on additional cHAP coating. (b) Cumulative, simultaneous BSA and lysozyme release from the system depicted in (a). (c–d) Cumulative release of (c) BSA encapsulated between cHAP coatings and (d) lysozyme bound on the additional cHAP coating (i.e. the outer layer of a layered cHAP coating).